Biosensors and Bioelectronics 272 (2025) 117083

Contents lists available at ScienceDirect

Biosensors and Bioelectronics

journal homepage: www.elsevier.com/locate/bios

Mid-infrared enhanced spectrochemical detection using azide vibrational probes

Valentina Di Meo [a,1], Gennaro Sanità [a,1], Angela Oliver [b,1], Annamaria Sandomenico [b], Massimo Moccia [c], Ivo Rendina [a], Alessio Crescitelli [a], Vincenzo Galdi [c], Menotti Ruvo [b,**], Emanuela Esposito [a,*]

[a] National Research Council (CNR), Institute of Applied Sciences and Intelligent Systems, I-80131, Naples, Italy
[b] National Research Council (CNR), Institute of Biostructures and Bioimaging, I-80131, Naples, Italy
[c] University of Sannio, Department of Engineering, Fields & Waves Lab, I-82100, Benevento, Italy

ARTICLE INFO

Keywords:
Surface-enhanced infrared absorption spectroscopy
Label free detection
Plasmonic biosensors
Small molecule detection
Vibrational probe

ABSTRACT

Spectrochemical analysis of trace elements in complex matrices is crucial across various fields of science, industry, and technology. However, this analysis is often hindered by background interference and the challenge of detecting ultralow analyte concentrations. Surface Enhanced Infrared Absorption (SEIRA) spectroscopy is emerging as a viable technique to address these challenges as it can successfully reveal soluble and unmodified analytes in a label-free manner through their interactions with a bioreceptor following site-specific labeling with small infrared-active probes. In this study, we present and demonstrate an advanced method for mid-infrared spectroscopy utilizing a pixeled SEIRA substrate coupled with a peculiar infrared-active vibrational probe. We select a small azide moiety as the vibrational tag since its signature around 2100 cm^{-1} is in the cell- and protein-silent window and its small size preserves the structure and biological function of the protein it integrates into. As model bioreceptor, we utilize an antigen-binding fragment (Fab') derived from the therapeutic antibody trastuzumab, modified with azidoacetic acid, and its Her2 antigen as the soluble analyte. Employing mid-infrared SEIRA spectroscopy, we are able to monitor the immobilization of the azide-modified Fab', and demonstrate the detection of analyte quantities as low as 83 amol within an area of 100 μm^2.

1. Introduction

Detecting trace substances in complex matrices in a label-free, real-time and non-invasive manner remains a significant challenge in analytical and pharmaceutical chemistry, as well as in environmental monitoring.

Despite the long-standing availability of techniques such as mass spectrometry-coupled chromatography (GC-MS and LC-MS (Beale et al., 2018; Wilson et al., 2024)), fluorometry (Zacharioudaki et al., 2022), colorimetry (Guo et al., 2024), surface plasmon resonance (SPR (Nguyen et al., 2015)) and biolayer interferometry (BLI (Petersen, 2017)), sensitivity issues persist for many analytes. Additionally, these methods often involve complex sampling and pretreatment processes, require expensive equipment, consume significant time and reagent, and necessitate very well trained operators (Kim et al., 2016; Steinhauser et al., 2012). Consequently, they are often unsuitable in terms of cost-effectiveness and environmental impact.

However, with the exception of SPR and BLI, these techniques offer the advantage of providing qualitative information essential for accurately identifying analytes. Similarly, Mid InfraRed (MIR) spectroscopy offers detailed insights into molecular structural properties through their distinctive vibrational features, which correspond to vibration frequencies within the MIR range of the spectrum (3300–600 cm^{-1} in wavenumber, or 3–25 μm in wavelength) (Chalmers et al., 2003; Stuart and Ando, 2004; Griffiths et al., 2007). MIR spectroscopy also enables quantitative analysis, in a real-time, label-free, simple, effective, and non-invasive manner (Pilling and Gardner, 2016), making it a promising technology for label-free biosensing.

* Corresponding author.
** Corresponding author.
E-mail addresses: menotti.ruvo@cnr.it (M. Ruvo), emanuela.esposito@cnr.it (E. Esposito).
[1] These authors contributed equally

https://doi.org/10.1016/j.bios.2024.117083
Received 28 August 2024; Received in revised form 6 December 2024; Accepted 18 December 2024
Available online 19 December 2024

Unfortunately, due to the very low molecular absorption cross-section of infrared vibrations ($\sigma_{abs} \sim 10^{-20}$ cm^2), as predicted by Beer's Law, MIR spectroscopy is inappropriate to detect trace analyte, severely limiting its applicability in sensitivity-demanding biochemical analyses.

The detection of target analytes can be significantly enhanced by leveraging the strong light-matter interactions facilitated by Localized Surface Plasmon Resonances (LSPRs) in metallic nanoantennas (NAs). A particularly powerful approach is the ultrasensitive Surface-Enhanced Infrared Absorption (SEIRA) spectroscopy (Neubrech et al., 2017; Wu et al., 2011; Adato et al., 2009), which utilizes resonant plasmonic metasurfaces (Chen et al., 2020). These metasurfaces consist of two-dimensional arrays of metallic NAs, carefully designed to align their LSPRs with the absorption bands of the target analyte (Brown et al., 2015; Brown et al., 2013; Dong et al., 2017; D'Andrea et al., 2013; De Tommasi et al., 2021). Within this context, collective effects arising from the periodic lattice also play a key role in enhancing the sharpness of the resonances (Adato et al., 2009). Such precise tuning amplifies the IR absorption cross-section by several orders of magnitude, enabling unprecedented sensitivity and the detection of analytes at extremely low concentrations.

To enhance the field in the very small volumes where the analyte is confined, SEIRA spectroscopy employs a two-dimensional array of NAs, tailored through *ad hoc* functionalized surfaces (Tanaka et al., 2022). This technique is gaining prominence in the field of biochemical analysis (Wang et al., 2024), offering unique advantages such as high sensitivity capable of detecting attomole-level quantities (Di Meo et al., 2021), and even single molecules (Ronen et al., 2015). Additionally, SEIRA provides the capability for *in-situ* and non-destructive monitoring of molecular fingerprint information in living organisms (Hui et al., 2021; Limaj et al., 2016; Yao et al., 2021).

Recent advances in nanofabrication and miniaturization have enabled SEIRA spectroscopy to detect multiple analytes through the design of specific surface structures, including pixeled metasurfaces (Di Meo et al., 2020; Leitis et al., 2019; Ma et al., 2015). In this approach, the metasurface is segmented in subregions or "pixels", each engineered to detect a specific vibrational frequency. This configuration allows a single chip or substrate to cover the entire frequency spectrum of interest, from the region of functional groups (between 4000 cm^{-1} and 1450 cm^{-1}) to the fingerprint region (between 1450 cm^{-1} and 500 cm^{-1}). By leveraging targeted functionalization techniques, SEIRA substrates can be tailored to detect and identify chemical species with unique IR signatures at extremely low concentrations, as well as to monitor the dynamics and kinetics of chemical reactions.

In this study, we explore the hypothesis that SEIRA substrates are effective for the label-free detection of any intact soluble analyte that is recognized and bound to the resonating interface by specific bioreceptors labeled with MIR probes. These probes exhibit resonances that are perturbed upon analyte binding. Functional groups that are IR active and resonate within specific IR spectral regions have the capacity to probe the nearest chemical environment, shedding light into intra- and inter-molecular interactions. These groups can be utilized for sensing purposes (Ma et al., 2015; Blasiak et al., 2017), as their IR signals predictably change in intensity and quality when they are located at the interface between the immobilized bioreceptor on the sensing surface and the interacting analyte.

IR-active functional groups possessing distinct spectroscopic IR signatures, such as metal carbonyls and nitriles, are valuable for probing the immediate chemical environment via specific inter-molecular interactions with their surroundings (Ma et al., 2015; Blasiak et al., 2017). By examining frequency shifts that occur due to variations in solvent exposure, or structural changes resulting from target binding or other biologically significant processes, it is theoretically feasible to detect modifications in the chemical environment around the IR probe, induced by conformational changes or perturbations arising from the proximity of interacting partners of the bioreceptor (Pazos et al., 2014; Shi et al., 2020).

The design of the IR probe is crucial for generating signals that resonate strongly in distinct and clean regions of the IR spectrum, enabling easier and more accurate monitoring of variations. Based on these considerations, and due to its small size and minimal structural impact upon integration, we opt for azide as the IR probe. Additionally, we select a Fab (fragment antigen-binding) with free cysteines at the C-terminus of the heavy chain as the bioreceptor to enable oriented and interaction-favorable anchoring to the gold NAs that constitute the metasurface. Specifically, we utilize a Fab' fragment derived from the therapeutic antibody trastuzumab as the bioreceptor and its antigen Her2 as the soluble analyte (Swain et al., 2023). Azidoacetic acid is chosen as an IR probe due to its resonance in a spectrum region devoid of intense signals from the antibody fragment or other biomolecules that may be present in the matrix (Adhikary et al., 2017). A key advantage of the technique is its suitability for monitoring metabolic processes while leveraging the benefits of multiplexed SEIRA Fourier-transform-IR (FTIR) spectroscopy. These include rapid acquisition of the full spectrum, enhanced absorption signals enabled by the SEIRA effect, and the ability to track reactions in real-time using the IR probe.

With this approach, we demonstrate the feasibility of monitoring the immobilization of the azide-modified Fab' using MIR SEIRA spectroscopy. Additionally, we observe a significant resonance shift of the probe upon binding of the bioreceptor to its antigen – a result that was not easily predictable. This finding opens avenues for designing similar biosensors where, by employing the appropriate bioreceptors, it becomes possible to detect any analyte in a label-free manner with exceptional sensitivity while maintaining qualitative control over the analyzed molecule.

2. Materials and methods

2.1. SEIRA substrate design

As schematized in Fig. 1, our SEIRA platform features a single substrate housing multiple metasurfaces ("pixels"). Each pixel consists of a two-dimensional array of cross-shaped gold NAs with precisely engineered geometrical parameters designed to resonate at specific MIR frequencies; an unpatterned area on the substrate serves as a reference (gold mirror).

In our electromagnetic modeling and design approach, we employed the finite-element-based commercial software COMSOL Multiphysics v. 5.1 (www.comsol.com). The geometry, illustrated in Fig. 2a, comprises cross-shaped gold NAs with thickness $t = 50\,nm$, and arm length and width L and W, respectively, arranged on a two-dimensional square lattice with a period of P. The NAs are situated atop a 5*nm*-thick chrome

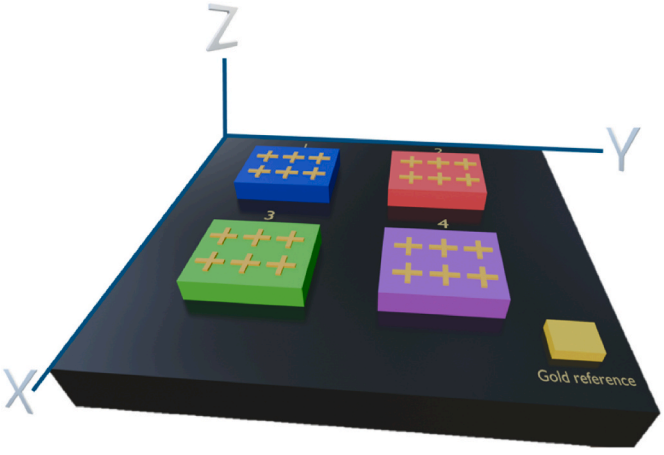

Fig. 1. Schematic of the pixeled SEIRA substrate.

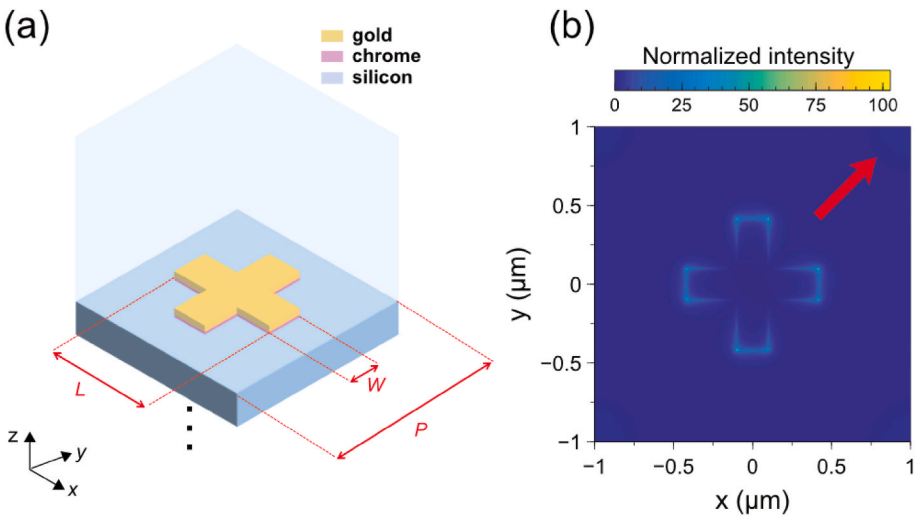

Fig. 2. (a) Schematic of metasurface unit cell. (b) Numerically computed intensity distribution (electric field, normalized with respect to the impinging one) within a unit cell, for pixel #3 (L = 835 nm, W = 200 nm, P = 2.0 μm) computed 5 nm away from the NA at the resonant wavenumber of 2035 cm^{-1}. The thick red arrow indicates the polarization of the impinging electric field (not aligned to the cross arms, for better visualization). (For interpretation of the references to color in this figure legend, the reader is referred to the Web version of this article.)

layer, which overlays a silicon substrate, all within an air environment. This particular geometry has proven effective in prior studies (Di Meo et al., 2020, 2021), demonstrating substantial field enhancement and polarization robustness.

To maintain computational efficiency, we adopted infinite periodicity in the transverse plane and assume normal incidence of a plane wave originating from the air region. This simplifies our analysis to a single three-dimensional unit cell (as shown in Fig. 2a), with periodic boundary conditions enforced on the lateral walls; this simulation setup captures both the LSPR and collective effects. Furthermore, we incorporated finite thicknesses for the air (10 μm) and substrate (5 μm) regions, implementing port-type and perfectly matched layer terminations, respectively.

To determine the material parameters, we employed the models in (Laman and Grischkowsky, 2008; Rakić et al., 1998; Li, 1980) for gold, chrome, and silicon, respectively. To discretize the computational domain, we employed standard meshing techniques with a maximum size of 10 nm, resulting in approximately eleven million degrees of freedom. Subsequently, we utilized the standard MUMPS solver with default parameters to obtain the frequency response.

To guide our design process, we conducted a thorough parametric exploration to identify resonances of interest within the geometrical parameter space. Fig. 2b displays a representative resonant-field distribution, revealing significant field enhancement (up to approximately three orders of magnitude; see Supporting Information) with hotspots at the arm tips, characteristic of plasmonic NAs. Subsequently, to achieve a resonance with the desired position and linewidth, we initiated the synthesis process with a coarse initial guess obtained from computed codebooks. Through iterative refinement of parameters, we fine-tuned the design to attain the desired response.

2.2. SEIRA substrate fabrication and characterization

The designed metasurface was transferred on a silicon chip using a fabrication process based on electron beam lithography (EBL) and lift-off process, as detailed in (Di Meo et al., 2019). The EBL process was performed on a 250 nm-thick polymethyl methacrylate (PMMA) resist. Following this, a 5 nm/50 nm chrome/gold stacked layer was deposited via DC sputtering. The lift-off process then removed the unexposed resist, realizing the designed metasurface.

In this experiment, the SEIRA substrate comprises four pixels fabricated on a 1cm × 1 cm silicon substrate. Each pixel, covering an area of 500 μm × 500 μm comprises an array of cross-shaped NAs with identical arm width (W = 200 nm) but varying arm lengths (L) and periods (P) to tune the plasmonic resonances within the functional group region, including one precisely targeting the IR probe signature around 2100 cm^{-1}. These nominal design values (summarized in Table 1) were selected after extensive testing to effectively capture the azide resonance. They were found to be optimal for detecting extremely low concentrations of such small molecules when bound to larger molecules.

As previously mentioned, adjacent to the pixels, a gold mirror covering an area of 200 μm × 200 μm was fabricated to serve as a reference mirror for IR spectroscopic characterization of the device. Each pixel is assigned a reference number, and their positions on the chip are identified using a Cartesian coordinate system, as illustrated in Fig. 1. The identification number, along with the Cartesian coordinates system, allows for easy and unique recognition of each pixel's position on the chip surface. To characterize the sensor surface and assess the fabrication quality, a scanning electron microscope (SEM) analysis was conducted. Fig. S1 in the Supporting Information presents a SEM image of a representative pixel (# 1), showing the expected geometrical parameters of the fabricated array.

After completing the morphological characterization, the IR spectrum of each array (in air) was measured. Reflection spectra were acquired using a Thermo-Scientific Nicolet iN10 MX FTIR instrument, with the reflection spectrum from the gold mirror serving as the reference background. A total of 256 scans were conducted at a resolution of 4 cm^{-1} within a 100 $\mu m \times 100\ \mu m$ window, covering the spectral range from 4000 to 650 cm^{-1}.

Table 1
Summary of geometrical parameters and corresponding plasmonic resonances of the fabricated device.

Pixel number	Geometrical parameters			ν_{exp} (cm^{-1})
	L [nm]	W [nm]	P [μm]	
#1	835	200	2.0	2090
#2	1030	250	1.5	1734
#3	1250	250	1.5	1553
#4	1120	250	2.0	1465

2.3. Preparation and characterization of azide-labeled trastuzumab Fab'

To obtain the azide-labeled Fab' of trastuzumab, we first generated the corresponding antibody F(ab')$_2$ (named Trast$_{Fab2}$, ≈100 kDa), by treating the full antibody with pepsin, following the method reported by Selis et al. (2016). The antibody's proteolytic fragment was purified to homogeneity by Size Exclusion Chromatography (SEC) on a Superdex S200 column (Cytiva, Milano, Italy) using phosphate-buffered saline (PBS) as the running buffer, and characterized by Liquid Chromatography-Mass Spectrometry (LC-MS) using an Orbitrap (Q-Exactive Plus) mass spectrometer coupled to an Ultimate 3000 HPLC (Thermo Fisher, Rodano, Italy). The system was equipped with a C4 Aeris column (Phenomenex, Castel Maggiore, Italy) equilibrated at 15% solvent B (CH_3CN, 0.05 % TFA) over solvent A (H_2O, 0.05 % TFA). To

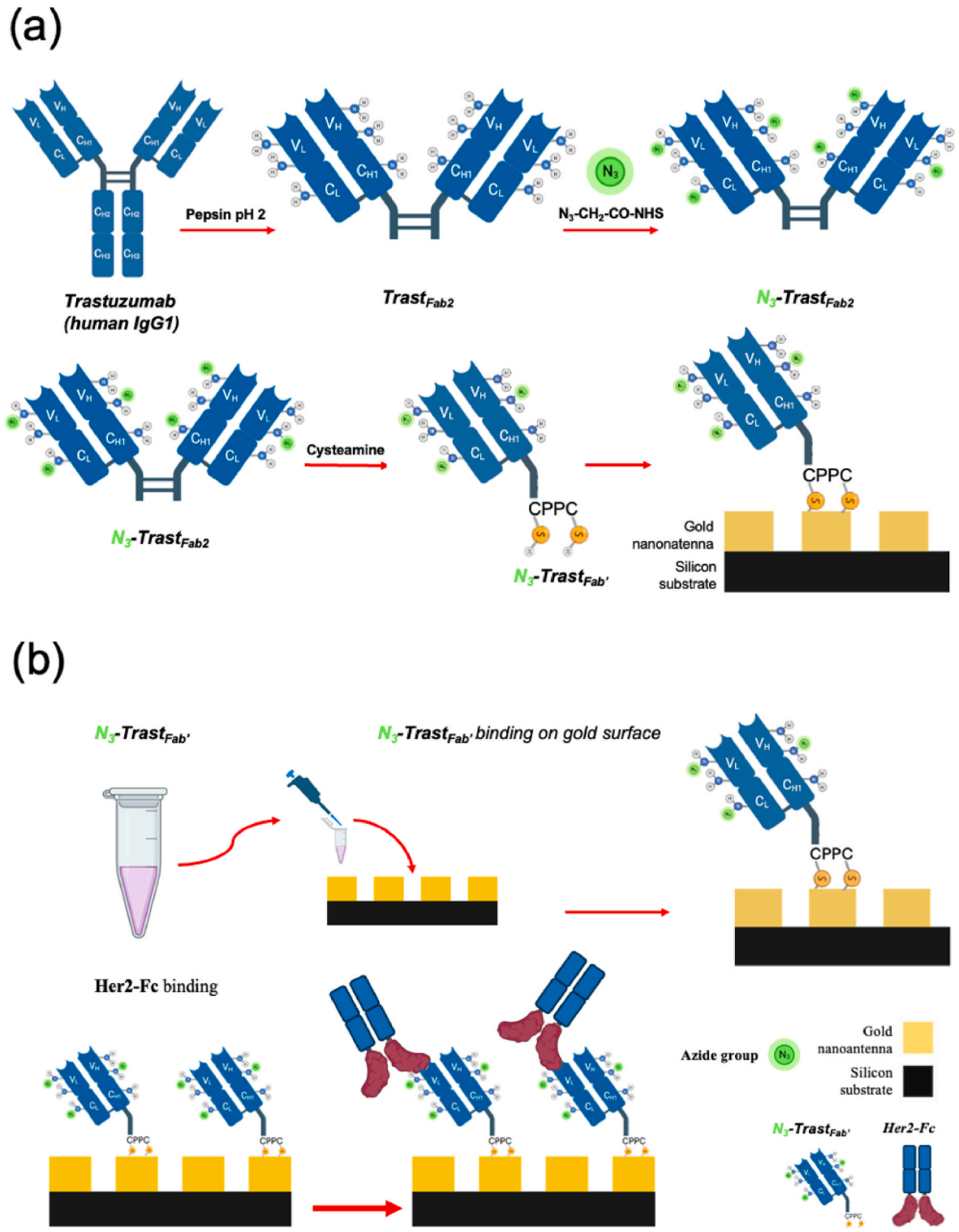

Fig. 3. (a) Schematic showing the preparation of the azide-modified Fab of trastuzumab. (b) Schematic of N_3-Trast$_{Fab'}$ coating on gold NAs and interaction with ErbB2-Fc. (For interpretation of the references to color in this figure legend, the reader is referred to the Web version of this article.)

elute the protein (300 ng), a gradient from 15% B to 70 % B was applied over 15 min at a flow rate of 0.2 mL/min. The mass spectrometer was operated in the positive ion mode, with the source at 350 °C and 3.5 kV, and auxiliary gas temperature of 100 °C. Three microscans with inject time 200 ms were averaged to obtain the final spectra. The RF was set to 150. Resolution was set to 17500. The m/z range was between 800 and 2400 m/z. Multicharged mass spectra were deconvoluted using BioPharma Finder vers. 5.1 (Thermo Fisher Instruments, Rodano, Italy) using the ReSpect algorithm for intact protein deconvolution. Proteins were analyzed by 12% Sodium Dodecyl Sulphate - PolyAcrylamide Gel Electrophoresis (SDS-PAGE) under native and reducing conditions. Concentration was determined spectrophotometrically on a Nanodrop 2000C instrument (Thermo Fisher Instruments, Rodano, Italy) using a $\varepsilon_{280nm} = 186000\ M^{-1}cm^{-1}$.

$Trast_{Fab2}$ (0.60 mg, 6 nmoles) was randomly labeled on the lysine side chains with azidoacetic acid by reacting the protein with a tenfold molar excess (1 mg/mL DMSO) of azidoacetic acid N-hydroxysuccinimide in 100 mM $NaHCO_3$ pH 8.3 for 1 h at 37 °C. The product was then reduced with cysteamine (MEA, Sigma-Aldrich, Milan, Italy (Selis et al., 2016)) to obtain the corresponding azide-modified monomeric $Trast_{Fab'}$ (molecular weight, MW ≈ 50 kDa), named N_3-$Trast_{Fab'}$, as shown in Fig. 3a. The final product was purified once more through SEC on a Superdex S200 gel filtration column, determining the concentration spectrophotometrically on a Nanodrop 2000C instrument using an $\varepsilon_{280nm} = 93000\ M^{-1}cm^{-1}$. To assess the extent of azide group incorporation, the product was finally analyzed by LC-MS under the conditions previously described for intact $Trast_{Fab2}$ analysis in the presence and absence of DTT (30 mM, 30 min, RT). The crystal structure of Her2 in complex with the Fab of trastuzumab (pdb id: 1N8Z) was visualized using PyMOL (The PyMOL Molecular Graphics System, Version 3.0 Schrödinger, LLC). Representative images of the antibody-antigen interface were generated using the same software.

Trastuzumab (also known by the trade name of Herceptin) aliquots were obtained, as reported by Selis et al. (2020). Carrier free recombinant human ErbB2/Her2 Fc chimera (hereafter Her2-Fc; Her2 residues Thr23-Thr652; cat. n. 1129-ER) and human VEGFR1/Flt-1 Fc chimera (aa 27–328, cat. n. 3516-FLL, hereafter VEGFR1-Fc) were obtained from R&D (Milano, Italy). This region of Her2 fused to Fc has an approximate MW of 96.8 kDa, 193.6 kDa considering a homodimer (https://www.rndsystems.com/products/recombinant-human-erbb2-her2-fc-chimera-protein-cf_1129-er), which is very similar to that of the actual soluble Her2 present in the blood circulation (Perrier et al., 2018). Azidoacetic acid N-hydroxysuccinimide was from Click Chemistry Tools (Scottsdale, AZ, USA).

2.4. SEIRA substrate functionalization

All pixels were initially cleaned by washing with isopropanol and double-distilled water to remove any potential contaminants. Surface biofunctionalization was conducted using the free thiol groups present on N_3-$Trast_{Fab'}$. N_3-$Trast_{Fab'}$ was treated with diluted Tris(2-carboxyethyl)phosphine (TCEP) (85 μM) for 60 min at room temperature to reduce the thiol groups on the heavy chain Cys229 and Cys232. These groups are susceptible to oxidation during handling, potentially restoring the $F(ab')_2$ or forming an internal cyclic disulfide bridge (Carrese et al., 2021). Subsequently, the solution was applied on the gold pixels (60 μL) and allowed to incubate for 60 min at room temperature. Following thorough washing with PBS and double-distilled water, the surface was dried under an N_2 flow. After collecting FTIR spectra, as described below in section 2.5, all pixels were exposed to Her2-Fc (3 μg/mL) in PBS (approximately 15 nM, considering the protein in the dimeric form) for 120 min at room temperature. Following extensive washing with PBS double-distilled water, pixels were dried again under an N_2 flow and subjected to FTIR analysis once more, as outlined in section 2.5. Fig. 3b illustrates a schematic of this process.

3. Results and discussion

We have designed, fabricated and tested a novel SEIRA-based sensing platform featuring an oriented bioreceptor labeled with a mid-IR active probe. This platform is capable of detecting specific analytes at extremely low concentrations and in a completely label-free manner.

The SEIRA substrate was engineered to detect an azide group, which is randomly attached on the bioreceptor's lysines and serves as a sensing probe for the captured analyte.

The azide group is particularly advantageous because its strong asymmetric stretching absorption occurs in the range 2167 to 2080 cm^{-1} (Pazos et al., 2014), which falls within the protein and cell-silent window (1700-2700 cm^{-1}) as shown in Fig. 4a, while the structure and the IR spectrum of azidoacetic acid are shown in Fig. 4b and c respectively. This makes azide an ideal tag, also because it is chemically inert at room temperature and in the absence of strong electrophiles, and is absent in naturally occurring living systems and biomolecules. Therefore, no interference from endogenous functional groups is expected, even in the presence of complex biological matrices. Due to its minimal toxicity and high biocompatibility, organic azide has already been used to monitor metabolic reactions (Prescher and Bertozzi, 2005). Its symmetric stretching absorption, which occurs at a considerably lower frequency (1343-1117 cm^{-1}) (Lieber et al., 1957), is much weaker and variable in position, making it unsuitable as a monitoring signal in sensing experiments.

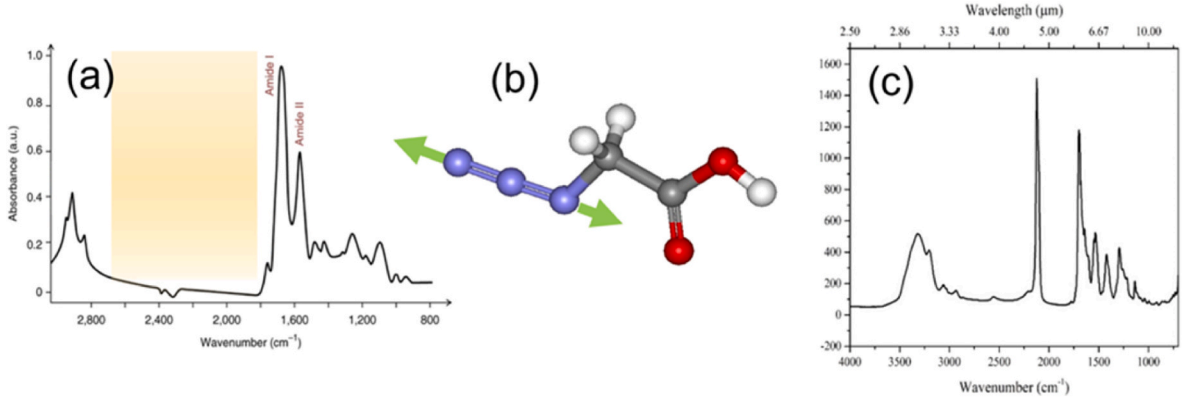

Fig. 4. (a) Typical IR absorption spectrum for biomolecules; the silent window (1700–2700 cm^{-1}), where no peaks from endogenous biomolecules are detected, is highlighted with orange shading. (b) Three-dimensional structure of azidoacetic acid: the azide group is shown in purple, the carbon atoms in red, the hydrogen atoms in white, and the oxygen atoms in red. The green arrows on the nitrogen atoms of the azide group visualize the asymmetric stretching vibrational modes ν_{asym} (N_3) of the chemical group. (c) IR spectrum of azidoacetic acid. (For interpretation of the references to color in this figure legend, the reader is referred to the Web version of this article.)

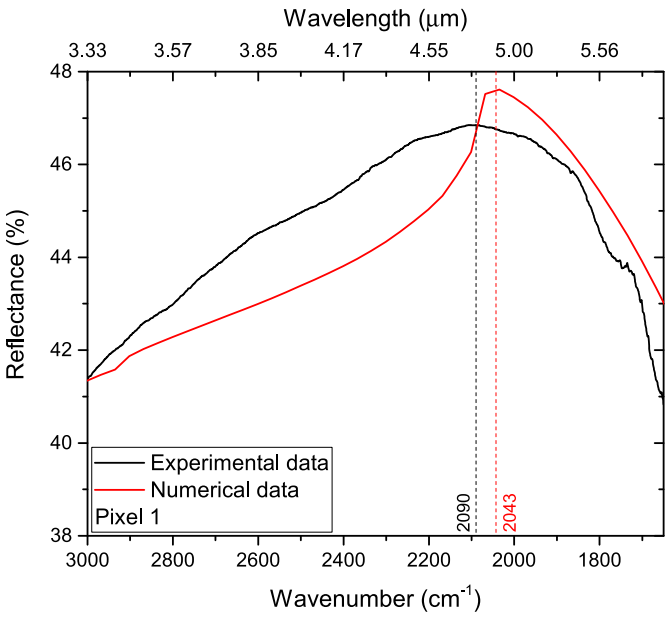

Fig. 5. Comparison between numerical (red curve) and experimental (black curve) reflectance responses pertaining to pixel #1 (L = 835 nm, W = 200 nm, P = 2.0 μm). (For interpretation of the references to color in this figure legend, the reader is referred to the Web version of this article.)

To experimentally validate the numerical model predictions, the IR spectra of each array in air were collected. Fig. 5 shows a comparison between the numerical (red curve) and experimental (black curve) data for a representative pixel (#1), demonstrating good agreement. The slight discrepancy between the curves can be attributed to fabrication tolerances, which are less than 5%. Similar results were observed for the other three pixels (see Figure S2–4 in the Supporting information).

Prior to surface functionalization, we conducted a thorough characterization of the azide-modified antibody bioreceptor to determine the degree of protein modification. $Trast_{Fab2}$, prepared by standard pepsin cleavage of the antibody, was highly pure as verified by SEC, SDS-PAGE (data not shown), and mass spectrometry analyses (refer to Figs. S5 and S6 in the Supporting Information). Similarly, N3-$Trast_{Fab'}$ appeared homogeneous based on SEC and SDS-PAGE analysis (Figs. S7a and b in the Supporting Information). LC-MS analyses under both reducing and non-reducing conditions revealed the heterogeneity expected from the random attachment of the azidoacetic moiety. This allowed for an estimation of the average number of azide copies incorporated into the antibody's light and pepsin-cleaved heavy chains. Fig. S8a indicates that one to three copies of azidoacetic acid (Δmass: 83.01 Da) were incorporated into N3-$Trast_{Fab'}$, with a predominance of antibody molecules with mono- and di-substitutions. Modifications affected both the light and heavy chains, as detailed in Figs. S8b and c.

We then conducted SEIRA analysis on the biosensor coated with the Fab fragment labeled with the IR probe. The presence of the antibody fragment was confirmed through the detection of vibrational bands from the amide bonds and the chemically introduced azide groups (Fig. 6a). Baseline-corrected reflectance spectra from a representative pixel (#1) revealed peaks at 2150 cm^{-1} (corresponding to azide asymmetric stretching absorption) and at 1750 cm^{-1} (attributed to the Amide I band of the protein), as shown in Fig. 6b. To assess the sensor's functionality, the azide-labeled Fab' was exposed to Her2-Fc to examine if the azide resonance was affected by the binding of the trastuzumab-specific antigen. After extensive washing to remove excess salts and Her2-Fc, the pixel resonance displayed a red-shift of 70 cm^{-1} (Fig. 6a, blue curve)

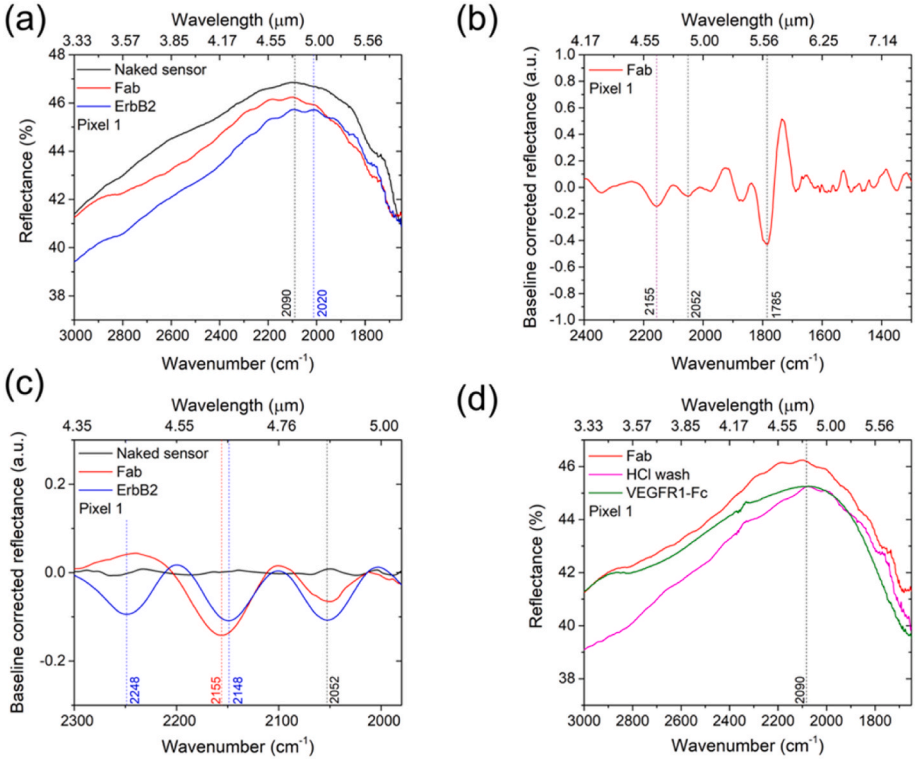

Fig. 6. FTIR reflectance measurements pertaining to pixel #1; (a) Black curve: reflectance resonance of naked substrate centered at 2090 cm^{-1}; red curve: reflectance resonance after Fab immobilization; blue curve: reflectance resonance after Her2-Fc binding. (b) Baseline-corrected reflectance with the detected molecular vibration, i.e., asymmetric stretching vibration of N3 ν_{antsy} at 2155 cm^{-1}. (c) Baseline-corrected reflectance resonance after Fab immobilization (red curve) and after antigen Her2-Fc binding, displaying a shift of 7 cm^{-1} for the asymmetric stretching relative to N3 group (blue curve). (d) Reflectance resonance after Fab binding (red curve), after washing in HCl to remove the bound antigen (pink curve), and after unrelated antigen VEGFR1-Fc incubation (green curve). (For interpretation of the references to color in this figure legend, the reader is referred to the Web version of this article.)

relative to the naked sensor (black curve). Additionally, the azide peak shifted by approximately 7 cm^{-1} in the presence of the antigen (Fig. 6c, blue curve). This shift suggests the potential of the azide groups to serve as a specific, albeit insofar qualitative, indicator of binding. Further peaks at 2249 and 2050 cm^{-1} were also observed, likely representing azide complexes with metal ions (2050 cm^{-1} (Di Bari et al., 2017)) and interactions with other low molecular weight components in the buffer (2246 cm^{-1}). To confirm that the azide band shift was specifically due to antigen recognition, we treated the sensor surface with HCl to dissociate bound Her2-Fc and reanalyzed it with SEIRA. The azide peak at 2150 cm^{-1} was restored after the treatment (Fig. 6d, pink curve), confirming that the shift was indeed antigen-mediated. Finally, to further validate the specificity of azide band shift, we exposed the sensor surface to a solution containing an unrelated antigen (VEGFR1-Fc), which has a similar molecular weight and Fc-mediated dimeric structure. Remarkably, the peak position remained unchanged (Fig. 6d, green curve), underscoring that the observed shift with the correct antigen was specific to the binding with the azide-labeled bioreceptor. The experiment was replicated on multiple substrates with identical pixel designs, and consistent results were obtained. An example is provided in the Supporting Information (Fig. S9).

These findings are based on measurements involving 2500 NAs, correlating with a 100 μm^2 area illuminated by the micro FTIR spectrometer. Given the number of gold atoms on each cross-shaped NA available for thiol bonding and the dimensions of a single Fab molecule (approximately 5 nm in cross-section and 7 nm in length), we estimate that each NA can accommodate up to 10000 (33 zmol) Fab molecules, i.e., 83 amol in 100 μm^2. If we assume a 1:1 binding ratio between the Fab and the antigen, it suggests that a similar quantity of analyte has been detected per NA in our experiments. Furthermore, since the Fab is only partially modified with the azide, the actual amount of antigen captured and detected is likely less than the equimolar ratio. While this study does not primarily focus on statistical metrics to quantitatively assess the sensor's performance, we have conducted a preliminary evaluation of its Limit of Detection (LoD). The LoD, defined as the lowest detectable concentration cL, corresponds to the smallest measurable signal x_L that can be reliably distinguished under a given analytical procedure. For our sensor, we estimate a LoD of 5 pM, as detailed in the supporting info; in the case of soluble Her2, this is well below the clinically significant threshold of 71 pM (15 ng/mL), calculated assuming a MW of around 210 kDa for to the dimeric soluble form of Her2 (Perrier et al., 2018).

The degree of molecule labeling can be a critical limitation in this type of experiment, making it crucial to carefully prepare and thoroughly characterize the bioreceptor before use. It is essential to avoid over-modification of the antibody fragment to prevent significant molecule distortion, which could impair antigen recognition. In our experiments, the level of azide modification was carefully controlled and proved to be adequate for selective antigen recognition, ensuring the sensor functioned correctly.

4. Conclusion

MIR and IR spectroscopies are essential for label-free detection. However, while these techniques excel qualitatively, they face limitations in detecting low concentrations and in studying dynamic metabolic pathways. Moreover, when working with biological samples, it is crucial to use specific probes to shift signals to protein- and cell-silent regions of the spectrum.

In this study, we have integrated the SEIRA effect, which enhances interaction between the IR field and vibrating molecules to boost sensitivity, with a biochemical platform incorporating an IR probe that enables the dynamic monitoring of biological and chemical events in its surroundings.

We have demonstrated the effectiveness of SEIRA substrates for label-free detection of intact soluble analytes, utilizing specific bioreceptors labeled with MIR probes that interact at the resonant interface. Upon analyte binding, the vibrational resonances of the probe undergo significant shifts, enabling both quantitative and qualitative monitoring of the interaction. We selected azide as the IR probe due to its signature residing in a region typically devoid of biomolecule interference, and its minimal impact on the receptor's structure and binding ability upon covalent integration. The bioreceptor used was an azide-modified Fab' fragment derived from the therapeutic antibody trastuzumab, with its antigen Her2 serving as the soluble analyte. Using our MIR SEIRA spectroscopy platform, we have demonstrated the capability to monitor the immobilization of the azide-modified Fab' and detect as little as 83 amol of analyte across a 100 μm^2 area. This versatile probe can be readily integrated into various biological molecules to selectively investigate their structural and environmental changes. The precise positioning and number of probe copies on the protein's outer surface are critical for effectively sensing its immediate surroundings while maintaining its functional integrity and interaction ability with analytes. We have employed an N-hydroxysuccinimide (NHS) derivative of azidoacetic acid, which modifies lysine and potentially histidine side chains or the N-terminus of a protein. While alternative reagents can link to other amino acid side chains, lysine's abundance on globular proteins and its surface localization make it particularly suitable for this application. Studying the distribution of lysine and controlling the extent of surface modification are crucial steps to balance the number of probe copies, enhancing sensitivity and the likelihood of establishing interactions without causing structural distortions that could deactivate protein function. In our case, examining the crystal structure of the trastuzumab Fab bound to the Her2 ectodomain (Pdb id: 1N8Z, Fig. S10 (Cho et al., 2003)), we observe that only three lysine residues on the Fab (Lys30, Lys65, Lys 76 on the heavy chain) are in close proximity with the Her2 interface. Based on the mass spectrum of the azide-modified Fab, it appears that at most one or two lysines can feasibly accommodate the probe and effectively sense the receptor. This suggests that very few copies of the azide moiety are sufficient to detect such a large analyte. However, detecting small analytes that cover limited contact surfaces on the bioreceptor may not be as straightforward, as they may not interact sufficiently with any of the IR probes. In such cases, it is essential to carefully study the interaction surface area of the bioreceptor and modify it in a site-specific manner to accommodate IR probes effectively. Importantly, our platform could significantly enhance the analytical capabilities of MIR spectral imaging (MIRSI) using SEIRA substrates (Rosas et al., 2023) as an advanced label-free method for chemical tissue imaging. It is noteworthy that we have demonstrated the functionality of the IR probe using a commercially available FTIR spectrometer accessible in any laboratory. Moreover, these probes can be readily adapted for other applications such as drug delivery schemes. By using different receptors with few copies of different probes, our detection platform has the potential to simultaneously sense and monitor multiple analytes at extremely low concentrations in a non-destructive and real-time manner.

In summary, the sensor system demonstrates the ability to detect virtually any analyte in a label-free manner with very high sensitivity, requiring minimal sample manipulation — merely dilution. A significant advantage of this approach lies in its rigorous quality control potential, enabled by the unique IR spectrum "fingerprint" of the analyte. Notably, while the bioreceptor chemically modified with the IR probe becomes part of the sensor itself, the analyte itself requires no labeling or modification for detection. The capability extends to analytes in diverse matrices without the need for pretreatment, paralleling the high sensitivity of techniques such as mass spectrometry. Furthermore, the system provides a dual advantage: label-free detection combined with cross-validation through the analyte's IR spectrum. These attributes (label-free operations, high sensitivity, and qualitative confirmation) position SEIRA as a highly promising technique, potentially surpassing established methods such as SPR or BioLayer Interferometry in power and versatility, and make it a valuable toolkit for chemical and biochemical analysis, environmental monitoring, pharmaceutical industry, and

thermal imaging applications.

CRediT authorship contribution statement

Valentina Di Meo: Writing – review & editing, Writing – original draft, Methodology, Investigation, Data curation. **Gennaro Sanità:** Writing – review & editing, Writing – original draft, Methodology, Investigation, Data curation. **Angela Oliver:** Methodology, Investigation, Data curation. **Annamaria Sandomenico:** Methodology, Investigation, Data curation. **Massimo Moccia:** Methodology, Investigation, Data curation. **Ivo Rendina:** Writing – original draft, Methodology, Investigation. **Alessio Crescitelli:** Writing – review & editing, Methodology, Investigation. **Vincenzo Galdi:** Writing – review & editing, Writing – original draft, Supervision, Methodology, Investigation, Data curation. **Menotti Ruvo:** Writing – review & editing, Writing – original draft, Supervision, Methodology, Investigation, Data curation, Conceptualization. **Emanuela Esposito:** Writing – review & editing, Writing – original draft, Supervision, Methodology, Investigation, Funding acquisition, Conceptualization.

Data availability

All code, simulation, and data files used to obtain the described results are available from the authors upon request.

Declaration of competing interest

The authors declare that they have no known competing financial interests or personal relationships that could have appeared to influence the work reported in this paper.

Acknowledgements

This work has been partially supported by the Italian National Research Council (CNR) through the project TIPPS (Tracking and Identification of asymptomatic Patients through engineered antibodies-bioconjugated plasmonics in a Pandemic Scenario) under Progetti@CNR 2020, and by the Italian Ministry of Research (MUR) through the project REMINDS (multi-REsonant Metasurfaces for enhanced INfra-reD Spectroscopy, code 20227MLENF) under the PRIN 20222 program.

Valentina Di Meo, Gennaro Sanità and Angela Oliver contributed equally to this work.

Appendix A. Supplementary data

Supplementary data to this article can be found online at https://doi.org/10.1016/j.bios.2024.117083.

Data availability

Data will be made available on request.

References

Adato, R., Yanik, A.A., Amsden, J.J., Kaplan, D.L., Omenetto, F.G., Hong, M.K., Erramilli, S., Altug, H., 2009. Ultra-sensitive vibrational spectroscopy of protein monolayers with plasmonic nanoantenna arrays. Proc Natl Acad Sci U S A 106, 19227–19232.

Adhikary, R., Zimmermann, J., Romesberg, F.E., 2017. Transparent window vibrational probes for the characterization of proteins with high structural and temporal resolution. Chem Rev 117, 1927–1969.

Di Bari, C., Mano, N., Shleev, S., Pita, M., A, L.D.L., 2017. Halides inhibition of multicopper oxidases studied by FTIR spectroelectrochemistry using azide as an active infrared probe. J. Biol. Inorg. Chem. 22, 1179–1186.

Beale, D.J., Pinu, F.R., Kouremenos, K.A., Poojary, M.M., Narayana, V.K., Boughton, B. A., Kanojia, K., Dayalan, S., Jones, O.A.H., Dias, D.A., 2018. Review of recent developments in GC-MS approaches to metabolomics-based research. Metabolomics 14, 152.

Blasiak, B., Londergan, C.H., Webb, L.J., Cho, M., 2017. Vibrational probes: from small molecule solvatochromism theory and experiments to applications in complex systems. Acc. Chem. Res. 50, 968–976.

Brown, L.V., Zhao, K., King, N., Sobhani, H., Nordlander, P., Halas, N.J., 2013. Surface-enhanced infrared absorption using individual cross antennas tailored to chemical moieties. J. Am. Chem. Soc. 135, 3688–3695.

Brown, L.V., Yang, X., Zhao, K., Zheng, B.Y., Nordlander, P., Halas, N.J., 2015. Fan-shaped gold nanoantennas above reflective substrates for surface-enhanced infrared absorption (SEIRA). Nano Lett. 15, 1272–1280.

Carrese, B., Cavallini, C., Sanità, G., Armanetti, P., Silvestri, Calì G., Pota, G., Luciani, G., Menichetti, L., Lamberti, A., 2021. Controlled release of doxorubicin for targeted chemo-photothermal therapy in breast cancer HS578T cells using albumin modified hybrid nanocarriers". Int. J. Mol. Sci. 22, 11228.

Chalmers, J., Griffiths, P.R., 2003. In: Chalmers, John, Griffiths, Peter R. (Eds.), Handbook of Vibrational Spectroscopy. John Wiley & Sons Ltd., Chichester.

Chen, W.T., Zhu, A.Y., Capasso, F., 2020. Flat optics with dispersion-engineered metasurfaces. Nat. Rev. Mater. 5, 604–620.

Cho, H.S., Mason, K., Ramyar, K.X., Stanley, A.M., Gabelli, S.B., Denney Jr., D.W., Leahy, D.J., 2003. Structure of the extracellular region of HER2 alone and in complex with the Herceptin Fab. Nature 421, 756–760.

D'Andrea, C., Bochterle, J., Toma, A., Huck, C., Neubrech, F., Messina, E., Fazio, B., Marago, O.M., Di Fabrizio, E., Lamy de La Chapelle, M., Gucciardi, P.G., Pucci, A., 2013. Optical nanoantennas for multiband surface-enhanced infrared and Raman spectroscopy. ACS Nano 7, 3522–3531.

Dong, L., Yang, X., Zhang, C., Cerjan, B., Zhou, L., Tseng, M.L., Zhang, Y., Alabastri, A., Nordlander, P., Halas, N.J., 2017. Nanogapped Au antennas for ultrasensitive surface-enhanced infrared absorption spectroscopy. Nano Lett. 17, 5768–5774.

Griffiths, P.R., de Haseth, J.A., 2007. Theoretical background. In: John Wiley & Sons, I. (Ed.), Fourier Transform Infrared Spectrometry. John Wiley & Sons, Inc., Chichester, pp. 19–55.

Guo, Z., Wang, X., Sun, H.L., 2024. A sensitive Ag(+)-mediated magnetic relaxation and colorimetry dual-mode sensing platform. Talanta 276, 126188.

Hui, X., Yang, C., Li, D., He, X., Huang, H., Zhou, H., Chen, M., Lee, C., Mu, X., 2021. Infrared plasmonic biosensor with tetrahedral DNA nanostructure as carriers for label-free and ultrasensitive detection of miR-155. Adv. Sci. 8, e2100583.

Kim, M.M., Parolia, A., Dunphy, M.P., Venneti, S., 2016. Non-invasive metabolic imaging of brain tumours in the era of precision medicine. Nat. Rev. Clin. Oncol. 13, 725–739.

Laman, N., Grischkowsky, D., 2008. Terahertz conductivity of thin metal films. Appl. Phys. Lett. 93, 051105.

Leitis, A., Tittl, A., Liu, M., Lee, B.H., Gu, M.B., Kivshar, Y.S., Altug, H., 2019. Angle-multiplexed all-dielectric metasurfaces for broadband molecular fingerprint retrieval. Sci. Adv. 5, eaaw2871.

Li, H.H., 1980. Refractive index of silicon and germanium and its wavelength and temperature derivatives. J. Phys. Chem. Ref. Data 9, 561–658.

Lieber, E., Chao, T.S., Rao, C.N.R., 1957. Improved method for the synthesis of alkyl azides. J. Org. Chem. 22, 238–240.

Limaj, O., Etezadi, D., Wittenberg, N.J., Rodrigo, D., Yoo, D., Oh, S.H., Altug, H., 2016. Infrared plasmonic biosensor for real-time and label-free monitoring of lipid membranes. Nano Lett. 16, 1502–1508.

Ma, J., Pazos, I.M., Zhang, W., Culik, R.M., Gai, F., 2015. Site-specific infrared probes of proteins. Annu. Rev. Phys. Chem. 66, 357–377.

Di Meo, V., Caporale, A., Crescitelli, A., Janneh, M., Palange, E., De Marcellis, A., Portaccio, M., Lepore, M., Rendina, I., Ruvo, M., Esposito, E., 2019. Metasurface based on cross-shaped plasmonic nanoantennas as chemical sensor for surface-enhanced infrared absorption spectroscopy. Sensor. Actuator. B Chem. 286, 600–607.

Di Meo, V., Crescitelli, A., Moccia, M., Sandomenico, A., Cusano, A.M., Portaccio, M., Lepore, M., Galdi, V., Esposito, E., 2020. Pixeled metasurface for multiwavelength detection of vitamin D. Nanophotonics 9, 3921–3930.

Di Meo, V., Moccia, M., Sanita, G., Crescitelli, A., Lamberti, A., Galdi, V., Rendina, I., Esposito, E., 2021. Advanced DNA detection via multispectral plasmonic metasurfaces. Front. Bioeng. Biotechnol. 9, 666121.

Neubrech, F., Huck, C., Weber, K., Pucci, A., Giessen, H., 2017. Surface-enhanced infrared spectroscopy using resonant nanoantennas. Chem Rev 117, 5110–5145.

Nguyen, H.H., Park, J., Kang, S., Kim, M., 2015. Surface plasmon resonance: a versatile technique for biosensor applications. Sensors 15, 10481–10510.

Pazos, I.M., Ghosh, A., Tucker, M.J., Gai, F., 2014. Ester carbonyl vibration as a sensitive probe of protein local electric field. Angew Chem. Int. Ed. Engl. 53, 6080–6084.

Perrier, A., Gligorov, J., Lefèvre, G., Boissan, M., 2018. The extracellular domain of Her2 in serum as a biomarker of breast cancer. Lab. Invest. 98, 696–707.

Petersen, R.L., 2017. Strategies using bio-layer interferometry biosensor technology for vaccine research and development. Biosensors 7.

Pilling, M., Gardner, P., 2016. Fundamental developments in infrared spectroscopic imaging for biomedical applications. Chem. Soc. Rev. 45, 1935–1957.

Prescher, J.A., Bertozzi, C.R., 2005. Chemistry in living systems. Nat. Chem. Biol. 1, 13–21.

Rakić, A.D., Djurišić, A.B., Elazar, J.M., Majewski, M.L., 1998. Optical properties of metallic films for vertical-cavity optoelectronic devices. Appl. Opt. 37, 5271–5283.

Ronen, A., Serap, A., Hatice, A., 2015. Engineering mid-infrared nanoantennas for surface enhanced infrared absorption spectroscopy. Mater. Today 18, 436–446.

Rosas, S., Schoeller, K.A., Chang, E., Mei, H., Kats, M.A., Eliceiri, K.W., Zhao, X., Yesilkoy, F., 2023. Metasurface-enhanced mid-infrared spectrochemical imaging of tissues. Adv. Mater. 35, e2301208.

Selis, F., Foca, G., Sandomenico, A., Marra, C., Di Mauro, C., Saccani Jotti, G., Scaramuzza, S., Politano, A., Sanna, R., Ruvo, M., Tonon, G., 2016. Pegylated

trastuzumab fragments acquire an increased in vivo stability but show a largely reduced affinity for the target antigen. Int. J. Mol. Sci. 17, 491.
Selis, F., Sandomenico, A., Cantile, M., Sanna, R., Calvanese, L., Falcigno, L., Dell'Omo, P., Esperti, A., De Falco, S., Foca, A., Caporale, A., Iaccarino, E., Truppo, E., Scaramuzza, S., Tonon, G., Ruvo, M., 2020. Generation and testing of engineered multimeric Fabs of trastuzumab. Int. J. Biol. Macromol. 164, 4516–4531.
Shi, L., Liu, X., Shi, L., Stinson, H.T., Rowlette, J., Kahl, L.J., Evans, C.R., Zheng, C., Dietrich, L.E.P., Min, W., 2020. Mid-infrared metabolic imaging with vibrational probes. Nat. Methods 17, 844–851.
Steinhauser, M.L., Bailey, A.P., Senyo, S.E., Guillermier, C., Perlstein, T.S., Gould, A.P., Lee, R.T., Lechene, C.P., 2012. Multi-isotope imaging mass spectrometry quantifies stem cell division and metabolism. Nature 481, 516–519.
Stuart, B.H., 2004. Spectral analysis. In: Ando, D.J. (Ed.), INFRARED SPECTROSCOPY: FUNDAMENTALS AND APPLICATIONS. John Wiley & Sons, Ltd Chichester, pp. 45–70.
Swain, S.M., Shastry, M., Hamilton, E., 2023. Targeting HER2-positive breast cancer: advances and future directions. Nat. Rev. Drug Discov. 22, 101–126.
Tanaka, T., Yano, T., Kato, R., 2022. Nanostructure-enhanced infrared spectroscopy. Nanophotonics 11, 2541–2561.
De Tommasi, E., Esposito, E., Romano, S., Crescitelli, A., Di Meo, V., Mocella, V., Zito, G., Rendina, I., 2021. Frontiers of light manipulation in natural, metallic, and dielectric nanostructures. La Rivista del Nuovo Cimento 44, 1–68.
Wang, J., Xie, Z., Zhu, Y., Zeng, P., He, S., Wang, J., Wei, H., Yu, C., 2024. Surface-enhanced infrared absorption spectroscopy (SEIRAS) for biochemical analysis: progress and perspective. Trends in Environmental Analytical Chemistry 41, 1–16.
Wilson, M., Al-Hamid, A., Abbas, I., Birkett, J., Khan, I., Harper, M., Al-Jumeily Obe, D., Assi, S., 2024. Identification of diagnostic biomarkers used in the diagnosis of cardiovascular diseases and diabetes mellitus: a systematic review of quantitative studies. Diabetes Obes. Metabol.
Wu, C., Khanikaev, A.B., Adato, R., Arju, N., Yanik, A.A., Altug, H., Shvets, G., 2011. Fano-resonant asymmetric metamaterials for ultrasensitive spectroscopy and identification of molecular monolayers. Nat. Mater. 11, 69–75.
Yao, Z., Zhang, Q., Zhu, W., Galluzzi, M., Zhou, W., Li, J., Zayats, A.V., Yu, X.F., 2021. Rapid detection of SARS-CoV-2 viral nucleic acids based on surface enhanced infrared absorption spectroscopy. Nanoscale 13, 10133–10142.
Zacharioudaki, D.E., Fitilis, I., Kotti, M., 2022. Review of fluorescence spectroscopy in environmental quality applications. Molecules 27.